

# Tracing the Galactic Anticenter Stellar Stream with 2MASS M Giants

Helio J. Rocha-Pinto, Steven R. Majewski, M. F. Skrutskie, Jeffrey D. Crane

*Department of Astronomy, University of Virginia, Charlottesville, VA 22903*

helio, srm4n, mfs4n, jdc2k@virginia.edu

## ABSTRACT

The recently discovered, ring-like structure just outside the Galactic disk in Monoceros is detected and traced among 2MASS M giant stars. We have developed a method to recover the signature of this structure from the distance probability density function of stars along a given line of sight. Its detection is possible even when the metallicity is unknown, provided that the structure is not too embedded in the disk. Application of this method reveals the presence of a large group of M giant stars at a Galactocentric distance of  $18 \pm 2$  kpc, over  $+36^\circ < b < +12^\circ$  and  $100^\circ < l < 270^\circ$ . Evidence that the stream extends to high negative latitudes is also found. That the structure contains M giants shows that it contains populations of at least an order of magnitude higher abundance than the  $[\text{Fe}/\text{H}] = -1.6$  mean metallicity previously reported for this system. The structural characteristics of the stellar stream as traced by M giants do not support the interpretation of this structure as a homogeneously dense ring that surrounds the Galaxy, but as a more localized structure, possibly a merging dwarf galaxy with tidal arms, like the Sagittarius dwarf galaxy.

*Subject headings:* Galaxy: structure – Galaxy: disk – galaxies: interactions

## 1. Introduction

The 2MASS database includes the first homogeneous, all-sky photometric survey of Milky Way stars and has already reshaped our understanding of the structure of our Galaxy and its satellite system (e.g., Skrutskie et al. 2001; Weinberg & Nikolaev 2001; Majewski et al. 2003, “M03” hereafter). A particular advantage of the NIR photometry in 2MASS is its ability to probe highly dust-obscured regions (Dutra & Bica 2001; Ivanov et al. 2002; Dutra et al. 2003). Thus, 2MASS has the potential to provide new insight into the structure of the

low-latitude stellar feature recently reported by Newberg et al. (2002, hereafter N02) near the Galactic anticenter in Monoceros, and further studied with optical analyses by Yanny et al. (2003) and Ibata et al. (2003; hereafter “Y03” and “I03”, respectively). These previous studies conclude that this highly obscured, low latitude structure spans a large swath across the sky, but is narrowly distributed in distance. I03 showed that the feature presents a very narrow main sequence, and, from Sloan Digital Sky Survey spectra of some apparent turn-off stars, Y03 conclude this population has  $[\text{Fe}/\text{H}] = -1.6 \pm 0.3$ .

However, in their study of 2MASS-selected M giants with  $J - K_s \geq 1.0$ , M03 show evidence (see, e.g., their Figure 14) for the Monoceros (“Mon”) feature at the same Galactic locations as found by N02. If the Mon structure contains a substantial population of M giants, then it must contain stars substantially more enriched than  $[\text{Fe}/\text{H}] = -1.6$ . In dereddened  $K_s$  magnitudes the Mon feature is a fluffy structure similar to that shown by N02 (see Figure 19 in M03), but is a more coherent, narrower feature when  $K_s$  magnitudes are converted to distances after assuming a color-magnitude relation (CMR) appropriate to the Sgr core, which is dominated by an  $[\text{Fe}/\text{H}] \sim -0.4$  population. This provides circumstantial evidence for the presence of a Mon population with an approximately similar mean  $[\text{Fe}/\text{H}]$  (at least for that population contributing M giants), because adopting a red giant CMR appropriate to a substantially different metallicity (Ivanov & Borissova 2002) would presumably translate to an inflated distance spread.

We explore the Mon 2MASS M giant density enhancement with a technique that isolates coherent spatial features of uncertain metallicity. This also allows us to increase the statistical sample of giants over that in M03 by probing to a lower RGB luminosity limit (bluer  $J - K_s$  color), and thereby trace the Mon feature over 230 degrees in length.

## 2. Data Selection and density functions

The NIR two-color diagram allows ready discrimination of M dwarfs and giants (Bessell & Brett 1988). Here we employ the same 2MASS M giant two-color selection used by M03, but expand our color range to include stars with  $0.86 < J - K_s \leq 1.10$ . This provides sufficient sample sizes to allow probes of individual  $4^\circ \times 4^\circ$  fields centered to  $|b| > 34^\circ$ . We have excluded photometry from the 51 ms 2MASS exposures, which creates a magnitude limit of  $K_s \gtrsim 8$  in our catalogue. The typical number of M giants in fields at each latitude range are 14-27 for  $|b| \approx 34^\circ$  and 51-395 for  $|b| \approx 14^\circ$ . Because our primary goal is to *detect* the presence of the Mon system and determine its length and orientation, analysis is limited to fields only mildly ( $E_{B-V} < 0.555$ ) reddened and minimally affected by bulge contamination; thus regions within  $|b| < 12^\circ$  and  $-54^\circ < l < +54^\circ$  are avoided.

Since we do not know the  $[\text{Fe}/\text{H}]$  of each M giant in our sample, their absolute magnitudes are uncertain. For ascertaining relative distances (and assuming a nearly monometallic population) we could work with very narrow color range samples to minimize the dispersion in derived distance modulus. However, such samples would have rather low M giant density, and larger sky areas would be needed to recover sample statistics, reducing our angular resolution.

Rather than make histograms of assumed single distance values, we use an alternative, more robust method to find structures within the database via a generalized representation for the stellar distance distribution: Each star distance is given by a probability density function with shape determined by the metallicity uncertainty of the star. The metallicity probability density function (“MPDF”),  $P([\text{Fe}/\text{H}])$ , gives rise to a probability density function for the absolute magnitude ( $M_{K_S}$ ) of each star, which, in turn, will be reflected in a distance probability density function (“DPDF”). From the transformation law of probabilities (Press et al. 1989), then

$$P(D|K_S, J - K_S) = P([\text{Fe}/\text{H}]) \cdot \left| \frac{d[\text{Fe}/\text{H}]}{dM_{K_S}} \right| \cdot \left| \frac{dM_{K_S}}{dD} \right|, \quad (1)$$

where  $P(D|K_S, J - K_S)$ , hereafter  $P(D)$ , is the DPDF for a given apparent magnitude  $K_S$  and  $J - K_S$ . The MPDF is certainly a complex function that depends on the line of sight. For simplicity, we approximate it by a single-peaked function. By doing this, we expect more easily to find structures having narrower metallicity and distance distributions than Galactic disk stars, which present broad distributions. The MPDF peak metallicity affects the scale of the distance distribution, but it will not destroy any preexisting stellar distance groupings.

We have adopted the metallicity-dependent CMR for K-M giants given by Ivanov & Borissova (2002). The MPDF was modeled as a Gaussian with  $\mu = -1.0$  dex and  $\sigma = 0.4$  dex, chosen as a compromise between the contribution by a relatively metal-rich population that we suspect exists in the structure and the  $-1.6 \pm 0.3$  dex metallicity quoted by Y03. The calculation of  $P(D)$  is done as follows. Given  $J$  and  $K_S$ , each  $[\text{Fe}/\text{H}]$  corresponds to a unique  $D$ , which is used to substitute the metallicity in the right side of Eq. 1. This is done by using Ivanov & Borissova (2002)’s  $[\text{Fe}/\text{H}](M_{K_S})$  relation and the distance modulus equation. The derivatives in Eq. 1 are also calculated from these equations. The individual DPDFs for each star are then summed to yield the density function along a given line of sight. The strength of the method is that by focusing on the DPDF, we can isolate the relative distance range with the highest expectation of stars.

We are interested in discovering at which distances the DPDF peaks for each stellar field. The examples in Fig. 1 demonstrate the general character of the DPDF: In general,

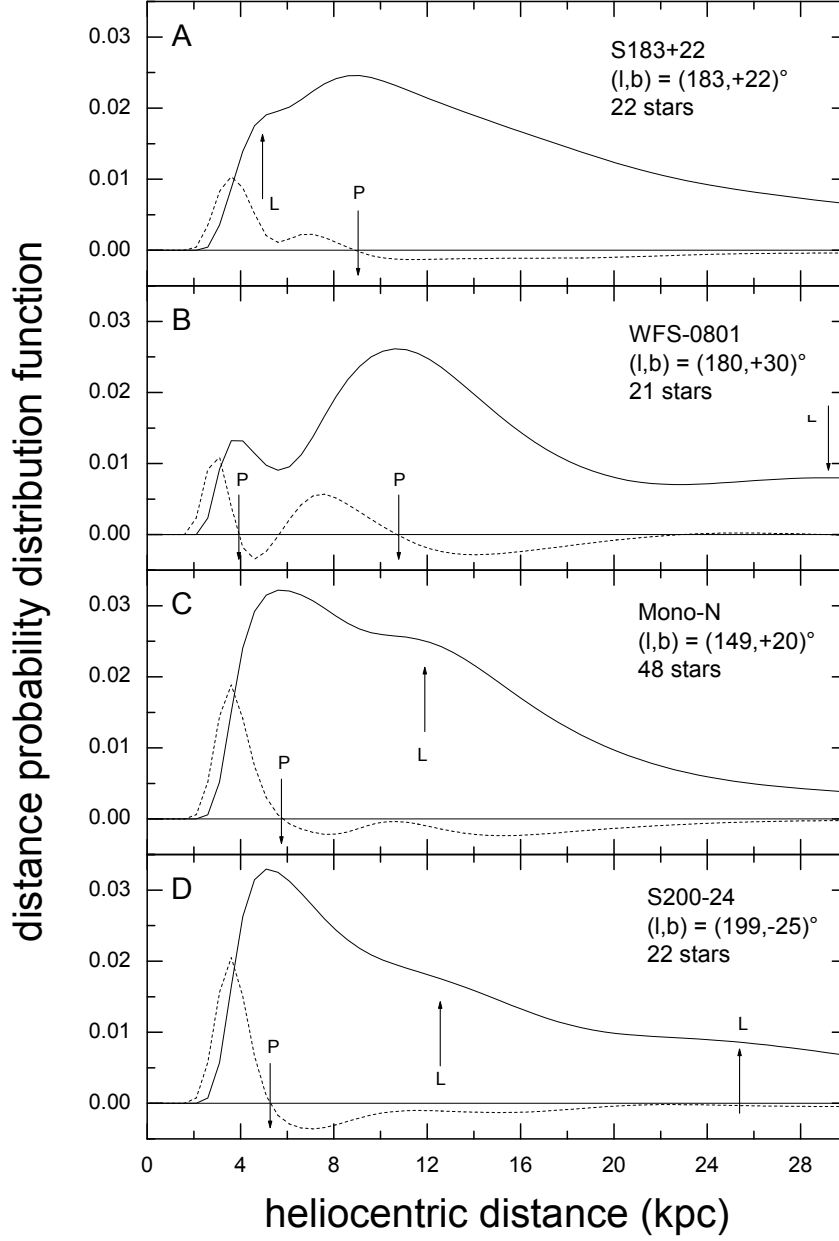


Fig. 1.— Definition of peaks and ledges in the DPDF for lines of sight centered at four stellar fields where the Mon structure has previously been found by I03 or Y03. A peak (labelled P) is a maximum value of the DPDF (global or local). Examples of ledges (labelled L) are also shown, although they are not used in the analysis. The first derivative of the DPDF (dashed lines) is used to find the position of the peaks. The presence of a peak (or ledge) between 9 and 13 kpc corresponds to our detection of the Mon structure in those fields.

a broad feature, corresponding to the disk, is found at nearby distances (that it peaks at typically 5-7.5 kpc is the result of missing bright M giants in our adopted 2MASS sample). In some lines of sight, a second farther peak (sometimes stronger than the first) is found between 9 and 13 kpc from the Sun. For other lines of sight, an underlying peak blends into the broader distribution, creating a “ledge”. These ledges also mark preferred stellar distances in the DPDF. Derivatives of the DPDF locate the position of peaks (Fig. 1) as global or local maxima of the DPDF. Though the ledges support the general trends as the peaks, due to our limited knowledge of the true density functions, we decided not to use the information provided by the ledges.

Two main features can be seen in a summary of the detections of peaks (Fig. 2). The large, closer strip comes from disk M giants, which only appear in our sample beginning at  $\sim 4$  kpc. The distance at which the bulk of disk stars appears is likely closer than shown, because thin disk stars are likely to be more metal rich than the adopted mean metallicity in the MPDF.

The other main feature in Fig. 2 is the secondary strip around 11 kpc away from the Sun. This strip is very obvious in the Northern Hemisphere. It corresponds to a preferred distance in the DPDF over a very large latitude range — from  $-36^\circ < b < +36^\circ$ , although at much less significance in the southern detections due to substantially more reddening in the Southern Hemisphere, which limited to a few the number of fields we explored there.

Beyond 20 kpc from the Sun, a much farther group of DPDF features is apparent in both hemispheres. While some could be related to real structures, the majority of the distant peaks reflect one or two stars that create bumps in the DPDF, and at present we cannot assure that they are real.

### 3. The Monoceros Stream

We identify the structure defined by the second strip of DPDF peaks in Fig. 2 as the Mon halo stream (N02, Y03), a.k.a. the One Ring (I03). This is shown in Fig. 1, where we give the M giant DPDF in  $4^\circ \times 4^\circ$  fields centered at  $(l, b)$  for four fields where it was identified. The bimodal PDFs in each panel indicate the existence of two distinct stellar groups.

Our results confirm the existence of this peculiar Galactic structure in the outskirts of the disk. Although the structure was first announced as a possible tidal stream, I03 have pointed to its very large size, arguing that it might be more properly interpreted as a stellar ring, forming the very distant edge of the disk. Fig. 1 confirms Ibata et al.’s findings in

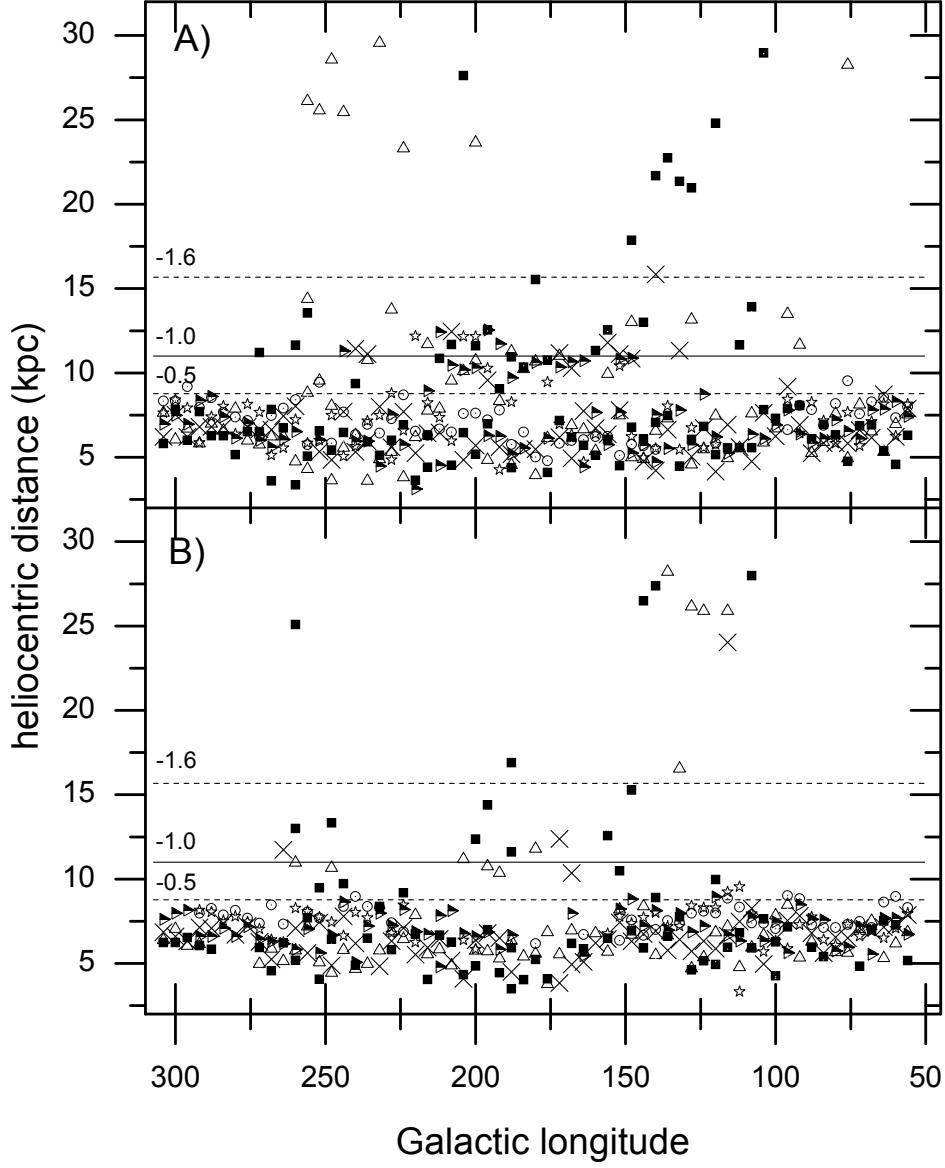


Fig. 2.— Heliocentric distances of the main DPDF features found. The symbol indicates the Galactic latitude of the  $4^\circ \times 4^\circ$  field for which a peak in the DPDF was found, as follows: solid squares,  $36^\circ$ - $32^\circ$ ; open triangles,  $32^\circ$ - $28^\circ$ ; crosses,  $28^\circ$ - $24^\circ$ ; half-filled right-pointing triangles,  $24^\circ$ - $20^\circ$ ; open stars,  $20^\circ$ - $16^\circ$ ; open circles,  $16^\circ$ - $12^\circ$ . A solid and two dashed horizontal lines indicate the mean distance of the feature we identify as the Mon structure for varying average [Fe/H] in the MPDF ( $-1.6$ ,  $-1.0$  and  $-0.5$  dex) as labelled in the plots. Panel A shows data for the North Galactic Hemisphere, panel B for the Southern Galactic Hemisphere.

specific fields they explored, and Fig. 3b shows that 2MASS traces the Mon feature over a large area of the sky. In the data that we have analysed, the signal of the structure is strongest over  $150^\circ < l < 220^\circ$ . From 20-30% of all M giants sampled in this area have most likely distances of 9-13 kpc. Closer to the Galactic plane, the structure is usually seen as a underlying peak (ledge) in the DPDF, due to the increasing dominance of disk M giants at smaller heliocentric distances.

In the North Hemisphere, peaks composing this structure have an average solar distance of  $11.2 \pm 0.11$  kpc, in general agreement with the 8-11 kpc reported by N02, Y03 and I03. Previous authors report the Mon structure to be more distant in the South Hemisphere. Although our detected Southern Hemisphere DPDF features do have a slightly larger distance ( $11.4 \pm 0.24$  kpc), they do not show as wide a north/south difference as reported earlier ( $\sim 2$  kpc). However, because we did not trace the structure as well in the south, the lack of substantial distance difference may not be significant.

When projected on the Galactic plane, the structure is remarkably well seen (Fig. 4). As in Fig. 2, the thick belt encircling the solar position gives the distance where the bulk of disk stars are found. Broadening of this belt is partly a projection effect and partly due to the poor match of the adopted MPDF to disk stars. The Mon structure appears as a generally thinner feature  $\sim 17.5 \pm 0.5$  kpc away from the Galactic center. The derived mean *heliocentric* distance (projected onto the Galactic plane) is nearly uniform over a great extent, from  $l = 130^\circ$  to  $210^\circ$ , but Fig. 4 conveys the impression that part of the structure may have significantly closer mean distance (perhaps even merging with the disk) in the third Galactic quadrant compared to the second. Based on the scatter of peaks, the Mon feature appears to be deeper around  $l = 200^\circ$ , but tapers to greater coherence for  $l < 195^\circ$ , reminiscent of a dwarf galaxy with attached tidal tail.

It is remarkable that although we have used an arbitrary MPDF, we have recovered stellar groups at the same position in the sky and nearly the same distance as those reported by N02, Y03 and I03. Tests show the thinness and distinctness of the Mon structure is remarkably robust to the adopted mean  $[\text{Fe}/\text{H}]$  of the MPDF, though, of course, the distance scale varies. The average distance of the structure is found to be approximated by

$$\langle d \rangle = d_0 (0.730 + 0.003[\text{Fe}/\text{H}] + 0.273[\text{Fe}/\text{H}]^2), \quad (2)$$

where  $d_0$  is the average distance when  $\langle [\text{Fe}/\text{H}] \rangle = -1.00$ . The effect of varying  $\sigma$  is more complex. With a broader MPDF, the DPDF both smears out and shifts to smaller heliocentric distances. This latter effect occurs because the metal-rich tail of the MPDF increases the probability of smaller distances for each star. A large  $\sigma$  would make nearly impossible the finding of an underlying blended peak, but the strongest features are still found: e.g., in the  $4^\circ \times 4^\circ$  field centered at  $(l, b) = (180^\circ, +30^\circ)$  (corresponding to I03's WFS-0801 field) the

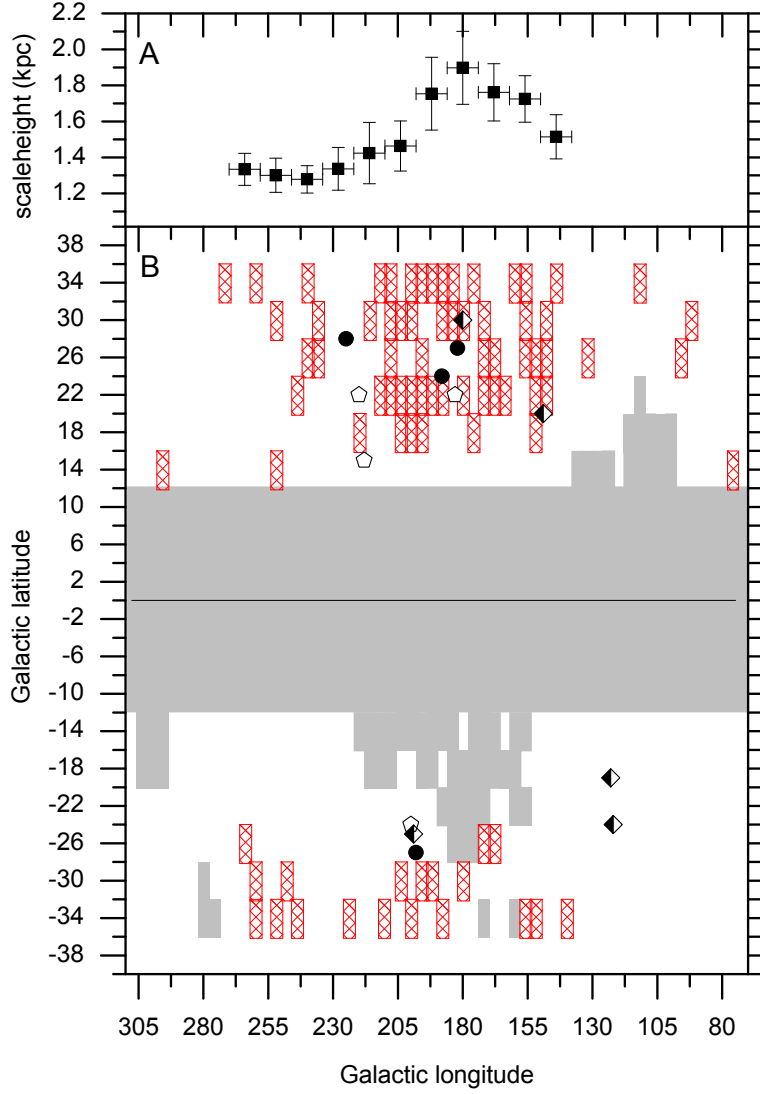


Fig. 3.— Spatial and vertical distribution of the Mon Structure. Panel A shows the variations in the scaleheight of the Mon structure, calculated from all stars with most likely distances of 9-13 kpc in the latitude range  $+12^\circ < b < +36^\circ$ . The structure seems to have a large vertical extent towards  $l \approx (180 \pm 6)^\circ$  and less towards  $l \approx (240 \pm 6)^\circ$ . Panel B shows the likely signatures of the Mon structure already found in the literature. The large gray area shows fields where our analysis was hindered by reddening. Filled rectangles indicate fields where a DPDF peak at heliocentric distances 9-13 kpc is found. Other symbols give the central coordinates of fields where the Mon structure was found previously: pentagon, N02 fields; circles, Y03 fields; half-filled diamonds, I03 fields. The apparent edge in the structure for  $|b| > 36^\circ$  is caused by the latitude cutoff of our analysis.



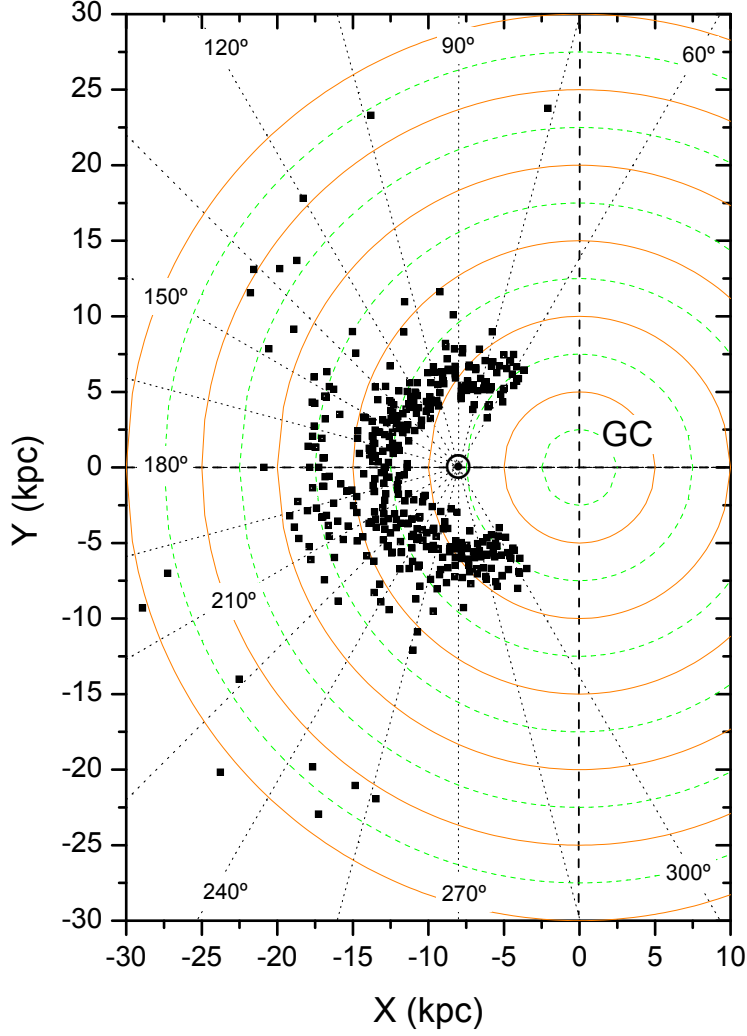


Fig. 4.— Projection onto the Galactic plane of Northern hemisphere DPDF signatures along different lines of sight. The Mon structure is the thin feature  $\sim 17.5 \pm 0.5$  kpc away from the Galactic center. Curves of galactocentric isodistances are shown as a guide. Galactic longitudes are indicated by dotted lines. The Mon structure seems to be thicker between  $195^\circ < l < 240^\circ$ , merging with the disk somewhere around  $l \approx 270^\circ$ .

Mon structure is found even with  $\sigma$  as large as 1.00 dex. The distance of each peak found has its own uncertainty, which depends on the broadness of the peak. From the fields we have surveyed, we estimate roughly that this error is, at most, 2 kpc. Additionally, there is the uncertainty coming from our choice of the average  $[\text{Fe}/\text{H}]$  of the MPDF, which is nearly 2 kpc, calculated from error propagation with Eq. 2. Adding these errors in quadrature, we have nearly a superior limit of 2.5 kpc for the average error in the distance of each peak.

In §1 we discussed previous evidence (M03) for the Mon feature in a sample of 2MASS M giants even redder than used here. The structure can be seen as a semi-detached blob centered at coordinates  $(-20, -7)$  kpc in Fig. 14e (and other panels of this figure) and  $(175^\circ, 11)$  kpc in the top panel of Fig. 10 in M03. This previous analysis uses a CMR derived from the Sagittarius core, expected to be dominated by  $[\text{Fe}/\text{H}] < -1$  stars, to assign a single distance to each star. Though a different approach to that undertaken here, the Mon structure nevertheless shows nearly the same distance even when M03’s redder stars ( $J - K_S > 1.10$ ) are considered. That the Mon feature is detected with even rather red M giants suggests the presence of a population substantially more metal-rich than reported by Y03 — a population as poor as their  $[\text{Fe}/\text{H}] = -1.6$  metallicity would have few tip giants in our sample and even less in M03’s reddest sample.

Taking the simplistic approach that all of the sampled stars with most likely distance between 9 and 13 kpc and  $140^\circ < l < 270^\circ$  are members of the structure, we calculate the mean scaleheight as  $1.3 \pm 0.4$  kpc. This value is very similar to the one calculated by Y03 ( $1.6 \pm 0.5$  kpc), but nearly two times larger than the scaleheight estimated by I03. However, because I03 adopted 8 kpc as the heliocentric distance of the structure, this will have shortened their scaleheight estimate by  $\sim 30\%$  relative to ours and Y03’s. Y03 points out that the scaleheight could be as high as 3 kpc. Our estimate is preliminary, since at the moment we cannot separate a minor contamination by disk and halo stars. For the Northern Hemisphere fields explored, the Mon structure seems to have a larger scaleheight (Fig. 3a) towards  $l \approx (180 \pm 6)^\circ$  and a smaller one towards  $l \approx (240 \pm 6)^\circ$ . Accounting also for the trend of lower scaleheight with decreasing  $l$  in the second quadrant, the collective density distribution bears the hallmarks of a larger core structure near  $l = 200^\circ$  with thinner, more coherent “tail” features in either direction.

Fig. 4, which gives the impression that the structure is arcing into the Galactic disk and merging with it beyond  $l \approx 270^\circ$ , suggests that the latter explanation is more likely. Moreover, in spite of being very large, Fig. 4 suggests that the structure also disappears at  $l < 90^\circ$ . On the other hand, inside  $-90^\circ < l < +90^\circ$  the 2MASS M giants begin to sample the inner Galaxy, and the disappearance of signatures of the Mon structure might also be explained by the preponderance of disk giants dominating the DPDF, making Mon peaks

progressively more difficult to see. In any case, the present analysis suggests that the Mon structure is not a uniform ring in terms of distance, depth, vertical extent or density.

Helmi et al. (2003) have analysed dynamical simulations of mergers for the creation of ring-like structures similar to Mon and discuss two possible scenarios for its origin that give rise to very different spatial distributions: (1) Recent accretion of a satellite galaxy in nearly coplanar orbit with the Galactic disk would form a transient arc of non-uniform Galactocentric distance. The feature would have a large number of stars and could obviously present a varying vertical distribution with respect to the Galactic equator. (2) An ancient minor merger would presently be seen as concentric shells around the Galaxy, symmetrically distributed with respect to the Galactic plane. Our results more strongly resemble the Helmi et al. models of the first situation: The Mon feature looks like a planar arc with a central core, greater coherence away from that core, and varying Galactocentric distance. Combined with the presence of relatively metal-enriched stars of the type expected in younger stellar systems, a tidally disrupted dwarf spheroidal scenario, similar to the Sgr system, seems most likely.

Although we have adopted the name Monoceros to this Galactic Anticenter structure, in order to be consistent with previous authors, we have found that the structure spans a large range of constellations. Since its center is yet unclear, other names may need to be considered after more data become available.

## REFERENCES

- Dutra, C. M. & Bica, E. 2001, *A&A*, 376, 434
- Dutra, C. M., Santiago, B. X., Bica, E. L. D., & Barbuy, B. 2003, *MNRAS*, 338, 253
- Helmi, A., Navarro, J. F., Meza, A., Steinmetz, M., & Eke, V. R. 2003, preprint (astro-ph/0303305)
- Ibata, R. A., Irwin, M. J., Lewis, G. F., Ferguson, A. M. N., Tanvir, N. 2003, accepted by *MNRAS* (astro-ph/0301067)
- Ivanov, V. D., Borissova, J. 2002, *A&A*, 390, 937
- Ivanov, V. D., Borissova, J., Pessev, P., Ivanov, G. R., & Kurtev, R. 2002, *A&A*, 394, L1
- Majewski, S. R., Skrutskie, M. F., Weinberg, M. D., Ostheimer, J. C. 2003, submitted (astro-ph/0304198)

- Newberg, H. J., Yanny, B., Rockosi, C. M., et al. 2002, ApJ, 569, 245
- Press, W. H., Teukolsky, S. A., Vetterling, W. T., Flannery, B. P., *Numerical Recipes in Pascal: The Art of Scientific Computing*, Cambridge Univ. Press, New York, 1989, p. 222
- Skrutskie, M. F., Reber, T. J., Murphy, N. W., & Weinberg, M. D. 2001, American Astronomical Society Meeting, 199,
- Weinberg, M. D. & Nikolaev, S. 2001, ApJ, 548, 712
- Yanny, B., Newberg, H. J., Grebel, E. K. 2003, et al. 2003, ApJ, 588, in press
- Yoss, K. M., Neese, C. L., and Hartkopf, W. I. 1987, AJ, 94, 1600